Journal of Cellular Biochemistry 97:869–881 (2006)

SCN^- Binding to the Charged Lysines of Histone End Domains Mimics Acetylation and Shows the Major Histone–DNA Interactions Involved in Eu and Heterochromatin Stabilization

Eligio Patrone,[1] Rosella Coradeghini,[2] Paola Barboro,[2] Cristina D'Arrigo,[1] Michele Mormino,[1] Silvio Parodi,[2,3] and Cecilia Balbi[2]*

[1]C.N.R., Istituto per lo Studio delle Macromolecole, Sezione di Genova, Via De Marini 6, 16149 Genova, Italy
[2]Istituto Nazionale per la Ricerca sul Cancro, Largo Rosanna Benzi 10, 16132 Genova, Italy
[3]Dipartimento di Oncologia, Biologia e Genetica, Università di Genova, Largo Rosanna Benzi 10, 16132 Genova, Italy

Abstract SCN^- binds to the charged amino group of lysines, inducing local changes in the electrostatic free energy of histones. We exploited this property to selectively perturb the histone–DNA interactions involved in the stabilization of eu and heterochromatin. Differential scanning calorimetry (DSC) was used as leading technique in combination with trypsin digestion that selectively cleaves the histone end domains. Euchromatin undergoes progressive destabilization with increasing KSCN concentration from 0 to 0.3 M. Trypsin digestion in the presence of 0.2 M KSCN show that the stability of the linker decreases as a consequence of the competitive binding of SCN^- to the amino groups located in the C and N-terminal domain of H1 and H3, respectively; likewise, the release of the N-terminal domain of H4 induces an appreciable depression in both the temperature and enthalpy of melting of core particle DNA. Unfolding of heterochromatin requires, in addition to further cleavage of H4, extensive digestion of H2A and H2B, strongly suggesting that these histones stabilize the higher order structure by forming a protein network which extends throughout the heterochromatin domain. J. Cell. Biochem. 97: 869–881, 2006.

Key words: chromatin structure; histone–DNA interactions; differential scanning calorimetry; eu and heterochromatin stability

A long-standing problem in cell biochemistry is the identification of the mechanisms by which chromatin condensation into higher order structures acts as a permanent repressor of gene expression [Weintraub, 1985]. Transmission electron microscopy of thin sections of resin embedded nuclei or cells visualizes condensed chromatin (heterochromatin) as electron dense domains anchored to the nuclear membrane or located in the perinucleolar region, suggesting that a gene close to a heterochromatin domain could be permanently inactivated through the spreading of heterochromatin along the DNA and its subsequent burying inside the condensed region. Reuter et al. [1990] have proposed earlier that this mechanism accounts for the position-effect variegation in *Drosophila* and a few years ago, in strong confirmation of this hypothesis, we noted that the increase in gene expression during the in vivo transformation of rat hepatocytes [Solt and Farber, 1976] is synchronous with an extremely large relaxation of condensed chromatin [Barboro et al., 1993]. This correlation was established by exploiting the extraordinary capability of differential scanning calorimetry (DSC) to distinguish between the condensed and the unfolded state

Grant sponsor: Fondo per gli Investimenti della Ricerca di Base (FIRB) (Project RBAUO1Y3SN); Grant sponsor: Ministero della Salute (2003-ICS conv. 137).

*Correspondence to: Cecilia Balbi, Istituto Nazionale per la Ricerca sul Cancro, Largo Rosanna Benzi 10, 16132 Genova, Italy. E-mail: cecilia.balbi@istge.it

Received 20 July 2005; Accepted 14 September 2005
DOI 10.1002/jcb.20689

of the genome [Nicolini et al., 1983]. Using DSC, we and other groups were indeed able to characterize the thermodynamics of salt induces condensation [Cavazza et al., 1991; Labarbe et al., 1996], to elucidate the mechanism of binding of H1 to core chromatin [Russo et al., 1995], to describe the all-or-none structural transition which occurs inside the chromatin loop [Balbi et al., 1999] and to identify the role of histone acetylation [Gavazzo et al., 1997] and of the nuclear envelope [Spadiliero et al., 2002], respectively, in the modulation of chromatin higher order structure.

It is apparent that, in order to attain a detailed molecular picture of heterochromatin dependent gene silencing or reactivation, several problems of increasing complexity must be addressed. In the first place, it should be borne in mind that the cooperativity of the transition between condensed and open states of chromatin likely plays a functional role in gene expression during development [Felsenfeld, 1996]. Recently, we were able to show, using the DSC approach, that chromatin condensation in native nuclei is confined to topologically closed domains (the loops) and involves an all-or-none structural change [Balbi et al., 1999]. These early observations on the occurrence of a first order transition have been interpreted within the frame of two different theoretical treatments based either on the cooperative binding of ligands to DNA [Teif et al., 2002] or on a physical model of chromatin as a tunable spring [Ben-Haïm et al., 2001].

Beside these advances in the theoretical modeling of chromatin phase transitions, the determination of the high (2.8 Å) resolution X-ray structure of the core particle [Luger et al., 1997] which, for the first time, specifies the positions of the N and C-terminal regions of histones, has very recently stimulated a rebirth of interest in basic structural aspect of chromatin folding. It is well known that 54 out of the 116 lysine residues contained in the nucleosome core particle are located inside the N-terminal tails of histones H2A, H2B, H3, and H4 and can establish electrostatic interactions with the DNA from the same or an adjacent nucleosome. Since these lysines undergo reversible acetylation/deacetylation and an acetylation step involves the loss of a positively charged group, it has been for a long time reported [van Holde, 1988] that histone acetylation represents a major local biochemical event in the process of modulation of the histone–DNA interactions. This hypothesis has been reexamined, very recently, in several detailed studies on the structural role of both intra and inter nucleosomal interactions of histone tails with DNA [Zheng and Hayes, 2003a,b].

The employment of DSC methods for the identification of the histone–DNA interactions involved in the stabilization of condensed chromatin is expected to usefully complement the results of X-ray crystallography. The principles of our DSC approach will be briefly outlined later on. Here, we recall that in the DSC profile of chromatin the heat adsorption peaks arise from the denaturation of DNA and/or histones inside energetically distinguishable (structural) domains. For example, the wrapping of DNA around the histone octamer in the core particle will cause ~150 bp to denature several degrees above the value of naked DNA, depending on the ionic strength [Cavazza et al., 1991]; any decrease (or increase) in the stability of the histone–DNA complex will, therefore, be directly reflected in the temperature and enthalpy of the endotherm. This effect suggests that the identification of the structural role of a specific interaction could be obtained, after selective perturbation of this latter, by the characterization of the changes in the DSC profile. The analysis of the modifications induced in the thermogram of chromatin by varying the monovalent electrolyte concentration allowed us to characterize the thermodynamics of the ionic strength dependent condensation process [Cavazza et al., 1991]. Unfortunately, simple electrolytes act, as a rule, as general structure perturbing agents, so that changes in local interactions cannot be evidenced. On the contrary, the anion SCN^- binds strongly and selectively to the NH_3^+ groups of the lysine side chains [Conio et al., 1974]; fully charged poly-L-lysine undergoes the coil to α-helix transition when the KSCN concentration is higher than 0.2 M, as a consequence of the strong charge suppression effect induced by the anion. Therefore, we reasoned that the binding of SCN^- to the charged amino groups located in the histone tails could mimic the specific weakening in the histone–DNA interactions induced by reversible acetylation–deacetylation.

In this study we relate, as far as possible, the conformational changes of chromatin with the specific dissociation of the histone tails from the DNA induced by SCN^- binding; this

effect has been evaluated using the extent of digestion with trypsin as a probe. Our results allow the identification of the major histone–DNA and histone–histone interactions involved in the stabilization of both the extended and condensed state of chromatin.

MATERIALS AND METHODS

Isolation of Nuclei From Rat Liver, Calf Thymus, and Chicken Erythrocytes

Rat liver, calf thymus, and chicken erythrocytes nuclei were obtained as already described. All of the isolation steps were carried out in dissociation medium (DM) (75 mM NaCl, 24 mM Na_2EDTA, pH 7.8) in order to prevent the activation of endogenous nuclease. Furthermore, all the buffers were supplemented with a mixture of protease inhibitors (5 mM Na_2SO_3, 1.2 mM phenylmethylsulfonyl fluoride (PMSF), 0.5 mM benzamidine, 25 μg/ml aprotinin). Shortly, hepatocytes were prepared from livers of male Fischer F-344 (Charles River, Como, Italy) following the procedure reported in Barboro et al. [1996]; nuclei were then isolated according to a continuous (in flow) method [Balbi et al., 1989]. A dilute (0.5×10^6 cells/ml) suspension of hepatocytes in DM, was mixed at 4°C with an equal volume of DM containing 1% (v/v) Triton X-100 by pumping into a small-volume mixing chamber and conveyed through a Teflon tube 0.1 cm in diameter and 100 cm long at a volume rate of flow of 1 ml/min. Nuclei were then recovered by centrifugation at 2,500*g* and the nuclear pellet equilibrated with the buffer used in the DSC determination. Nuclei from calf thymus were isolated according to Cavazza et al. [1991]. Twenty grams of frozen tissue were homogenized in a Waring blender with 300 ml of DM. The suspension was filtered through six layers of sterile gauze, and an equal volume of DM containing 0.6% (v/v) Triton X-100 was added under gentle shaking. After a 5 min incubation, nuclei were harvested by centrifugation at 500*g* for 10 min and resuspended in DM; this step was repeated three more times. Purified nuclei were recovered by centrifugation at 10,000*g* for 15 min, equilibrated with the buffers used in the DSC determinations or in the digestion experiments with micrococcal nuclease (MN) and trypsin. Erythrocyte nuclei were prepared as described by Labarbe et al. [1996]. Blood collected from freshly chickens was filtered on sterile gauze and dissolved in 1.5 vol of citrate buffer (0.76% sodium citrate, 1% D-glucose, pH 7.4). The solution was centrifuged at 900*g* for 20 min. The pellet was repeatedly washed with DM containing 0.5% (v/v) Triton X-100 and then centrifuged at 5,000*g* for 15 min until hemoglobin was completely extracted as judged from the color of the pellet. The pellet was washed several times with DM under the same conditions and resuspended in the buffers used in the DSC experiments.

Ionic Strength Conditions for the Observation of the Perturbing Effect of SCN^-

To characterize the effect of SCN^- binding on the DSC profiles of nuclear chromatin, DSC experiments were carried out in a wide (from 10 mM to 0.6 M) range of KSCN concentration. At low ionic strength, however, the electrostatic free energy of DNA increases abruptly, resulting in chromatin unfolding. This polyelectrolyte effect, which obscures the specific changes induced by SCN^-, is almost completely suppressed in 0.1 M monovalent salt. Therefore, for buffers containing 24 mM Na_2EDTA and 10 or 50 mM KSCN, the cation concentration was kept equal to that of DM (0.123 M) by adding the appropriate amounts of NaCl; for higher concentrations of KSCN the addition of NaCl was omitted. Aliquots of nuclear suspension where incubated for 1 h at 4°C at the same concentration of KSCN used in the calorimetric experiments, washed three times with the incubation buffer and then used for histone analysis.

Micrococcal Nuclease and Trypsin Digestion of Calf Thymus Nuclei

In the digestion experiments with MN (Sigma, St. Louis, MO) nuclei were resuspended in 80 mM NaCl, 10 mM Tris-HCl, pH 7.5, 1 mM $CaCl_2$ at a concentration of 30 mg/ml (corresponding to ~1.5 mg/ml of DNA) and digested with 20 U/ml MN at 37°C for 15 min. The digestion was stopped by adding an equal volume of 50 mM Na_2EDTA, 20 mM NaCl, 10 mM Tris-HCl, pH 7.5. In some experiments the digestion was carried out in the presence of 0.2 M KSCN; in this case 50 U/ml MN for 1 h were used.

For trypsin digestion calf thymus nuclei were resuspended at a concentration of 10 mg/ml in DM and digested with 100 μg/ml trypsin (Sigma) for 80 min or 15 μg/ml for 15 h at 4°C. The digestion was stopped by adding a fourfold excess of soybean trypsin inhibitor (Sigma). In

some experiments the digestion was carried out in the presence of 0.2 M KSCN.

Electrophoretic Characterization of the DNA Fragments and of the Histone Complement

After digestion with MN, DNA was isolated from nuclei with proteinase K followed by extraction with phenol and chloroform [Maniatis et al., 1982] and electrophoresed on 1.5% agarose gels in 90 mM Tris borate, pH 8.0, 2 mM Na_2EDTA. The gels were stained with 1 μg/ml ethidium bromide.

In order to evaluate the eventual loss of histones associated with the exposure of chromatin to KSCN in the range 10 mM–0.6 M, the histone complement was recovered from nuclear pellet by acid extraction followed by ethanol precipitation [Panyim et al., 1971] and run on 16% sodium dodecyl sulfate–polyacrylamide gel (SDS–PAGE) according to Laemmli [1970]. After staining with Coomassie brilliant blue the amounts of histones were determined by scanning the gels as already reported [Cavazza et al., 1991; Russo et al., 1995]. The same procedure was used to evaluate the fraction of trypsinized histones. The histone loss was evaluated using the electrophoresis of the native histone complement as the standard; in some cases the results were compared with those obtained by determining the fraction of tryptic digestion products. This method allows an accurate determination of the extent of digestion of each histone (limits of the SD ±2.5%).

DSC Determinations

DSC of purified nuclei was performed as already described [Balbi et al., 1989] with a Perkin-Elmer DSC7 microcalorimeter (Norwalk, CT) at a scan rate of 10°C /min. Deconvolution of the excess heat capacity curves was performed using the Microcal (TM) Origin 6.0 program.

RESULTS AND DISCUSSION

Structural Attribution of the Major Endotherms in the DSC Profile of Nuclei From Resting Cells: A Brief Re-Examination

In Figure 1, we report the scans of nuclei isolated from rat liver (a, b), chicken erythrocytes (c, d), and calf thymus (e, f): the major endotherms are marked by Roman numerals. On eye inspection the thermal profiles appear to be almost superimposable; minor differences,

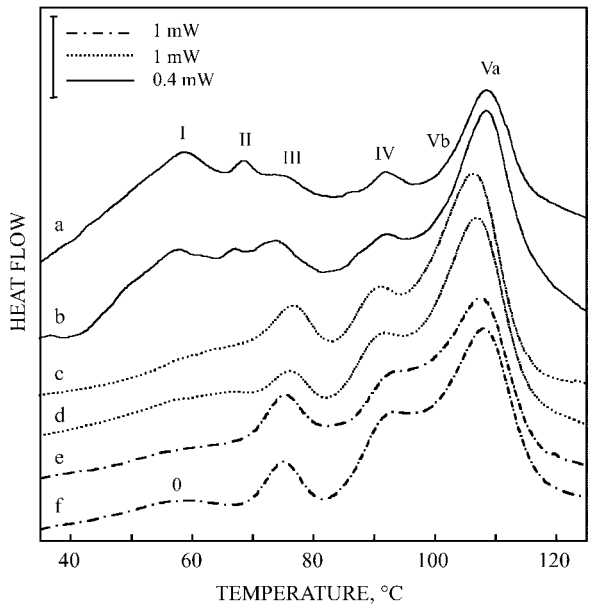

Fig. 1. Universal character of the thermal profile of chromatin from resting cells. Comparison among the thermal profiles of nuclei isolated from rat hepatocytes (**a**, **b**), chicken erythrocytes (**c**, **d**), and calf thymocytes (**e**, **f**). The major endotherms corresponding to the denaturation of histones or DNA inside the structural domains of chromatin are marked by Roman numerals. Transitions I and II in rat liver nuclei arise from the melting of residual intermediate filament proteins and of the nuclear matrix, respectively [Balbi et al., 1989]. Transition V_b at ~100°C is reproducibly observed after deconvolution of the thermal profiles.

mainly located between 90 and 110°C, reflect some variability between preparations of the same material, rather than minor but significant features of nuclei from different tissues. Since chromatin corresponds to about 90% of the dry weight of the nucleus the melting of other less abundant macromolecular components cannot, as a rule, be identified by our procedure; only in the case of rat hepatocytes (thermograms a and b) residual cytoskeletal filaments and the nuclear matrix give rise to two well detectable endotherms (endotherms I and II at 58 and 65°C, respectively) [Balbi et al., 1989]. Thus, the thermal profile can be regarded as the thermodynamic fingerprint of chromatin in resting cells. Additional data, further supporting this contention, are reported in Figure 2B, which shows that the dependence of the denaturation temperature of the structural domains of chromatin on KSCN concentration is the same for all the cell types examined. This "universal" character reflects the regular wrapping of the DNA around the

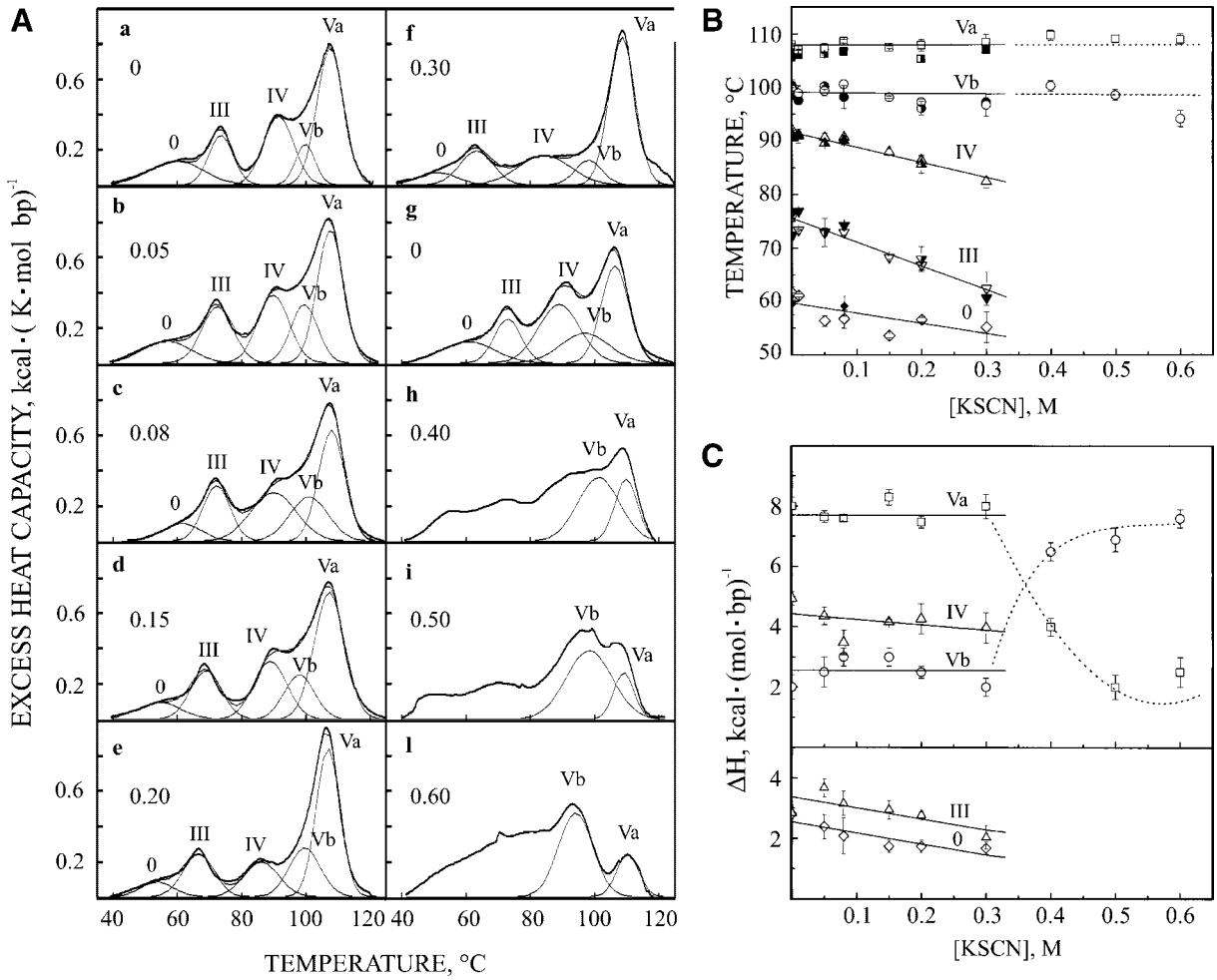

Fig. 2. Selective destabilization of euchromatin induced by SCN^- binding. **A**: The effect of SCN^- on the thermal profile of calf thymus nuclei. The excess heat capacity curves have been deconvolved into gaussian component transitions, marked by Roman numerals; the concentration of KSCN in mol/L is reported on the left of each panel. The dependence of the denaturation temperature (**B**) and enthalpy (**C**) of histones (endotherm 0) and of DNA (endotherms III, IV, V_b, and V_a) in the different structural domains of chromatin for calf thymus nuclei on KSCN concentration; the results obtained for nuclei from other resting cells have been reported for comparison in B. Full symbols, chicken erythrocytes; half-full symbols, rat hepatocytes; empty symbols, calf thymocytes. The points represent the mean ± SE of three to six determinations. The dotted lines in (B) and (C) evidence the conversion of heterochromatin (transition V_a) into the 30 nm fiber (transition V_b) which occurs as a consequence of the irreversible dissociation of chromatin induced by KSCN beyond 0.3 M.

histone octamer as well as the folding of the polynucleosomal chain into higher order structures.

For the purpose of an immediate appreciation of the data reported in this section it is appropriate to recall briefly the major outcomes of the DSC analysis of chromatin in situ. (1) The organization of the polynucleosomal chain into sharply defined structural domains causes the DNA to melt into two well separated thermal transitions at ~75 and ~90°C, corresponding to the denaturation of linker and core particle DNA, respectively; they are marked by III and IV in the thermograms of Figure 1. (2) Using DSC in combination with infrared spectroscopy, we were able to show that the histone globular domain melts in transition 0 [Cavazza et al., 1991]. The stabilization of the core particle DNA inside compact heterochromatic domains results in a new strong endotherm at ~107°C (V_a); another endotherm (V_b), corresponding to the denaturation of core particle DNA in a looser higher order structure, is reproducibly observed at ~100°C after deconvolution of the thermogram (Fig. 2A). We have recently demonstrated [Balbi et al., 1999] that tight aggregates of 30 nm fibers (heterochromatin) give rise to the 107°C transition, while isolated or loosely aggregated

fibers denature in endotherm V_b. (3) Chromatin decondensation induced by different agents results in the conversion of V_a into V_b and IV and vice versa [Cavazza et al., 1991]. This conversion is an athermal process, confirming that the structural domains are stabilized by entropy driven electrostatic interactions between histones and DNA. For this reason the fraction of condensed chromatin can be simply obtained by dividing the denaturation enthalpy of the transition V_a ($\Delta H_m^{V_a}$) by the total denaturation enthalpy ($\Delta H_m^{IV} + \Delta H_m^{V_b} + \Delta H_m^{V_a}$).

It is worth noting that the stability of the linker is only marginally affected by the process of condensation per se. The ionic strength dependent decondensation of calf thymus chromatin between 0.123 M and 1 mM Na^+ involves a limited, but reproducible (3°C), increase in T_m^{III}, which can be related with the transition from the more restrained state present in the higher order structure to the straight conformation which is characteristic of the extended polynucleosomal chain at low salt [Russo et al., 1995].

Selective Destabilization of Euchromatin by SCN^- Binding

Exhaustive thermodynamic analysis of the changes in the denaturation profile of nuclear chromatin induced by SCN^- has been carried out in the case of calf thymus nuclei. Representative thermograms, deconvolved into gaussian components, are reported in Figure 2A. In Figure 2B the peak temperatures (T_m) observed for calf thymus nuclei are plotted as a function of KSCN concentration; as reported above, also the values determined for rat liver and chicken erythrocyte nuclei have been included for comparative purpose. The stability of euchromatin decreases sharply with increasing SCN^- concentration compared with that of heterochromatin. A progressive flattening of the thermal profiles occur below ~95°C when the salt concentration is raised upto 0.3 M. The values of T_m^{III} and T_m^{IV} (Fig. 2B), as well as of ΔH_m^{III} and ΔH_m^{IV} (Fig. 2C), which represent a measure of the stability of the linker and of core DNA in euchromatin, show a large dependence on SCN^- concentration; $\Delta T_m/\Delta$[KSCN] for transitions III and IV is ~−39 and ~−28 deg/M, respectively. All of the changes are reversible; after re-equilibration of the chromatin samples with DM the thermal profile of native chromatin is regained (Fig. 2A, panel g). On the contrary, neither T_m^{Va} and ΔH_m^{Va} nor T_m^{Vb} and ΔH_m^{Vb} are appreciably affected between 0 and 0.3 M, showing that the interactions between core particles, which stabilize both heterochromatin and the 30 nm fiber [Russo et al., 1995], are not significantly loosened. Within this range the ratio ($\Delta H_m^{Va}/\Delta H_m^{IV} + \Delta H_m^{Vb} + \Delta H_m^{Va}$) apparently increases from 0.53 to 0.57 as a consequence of the decrease of ΔH_m^{IV}, suggesting an increase in the fraction of heterochromatin. This change, however, merely reflects, as already observed [Chipev and Angelova, 1983; Cavazza et al., 1991], the dependence of ΔH_m on T_m. Indeed ΔH_m for both long (~8,000 bp) and core particle DNA depends linearly on the temperature. The slope is equal to the difference between the heat capacities of the native and denatured state, respectively.

Since the structural effect of SCN^- might depend on histone dissociation rather than on the reversible suppression of stabilizing electrostatic interactions, we have checked our chromatin samples for the occurrence of histone loss. The electrophoretic pattern reported in Figure 3A shows that the amounts of histones that remain bound to DNA, when KSCN concentration is increased from 0 to 0.3 M (lanes 1–7), do not undergo any decrease, within the experimental error, with respect to native calf thymus chromatin. We next attempted to detect alterations of the nucleosomal repeat length using MN digestion as a probe; nuclei were incubated in digestion buffer or in digestion buffer containing 0.2 M KSCN as described in "Materials and Methods"; DSC experiments were carried out under the salt conditions used for digestion. Representative results are shown in Figure 3B. As already reported [Balbi et al., 1989] in digestion buffer (thermal profile a) transition V_a disappears, while endotherm IV at 88°C dominates the thermogram; T_m^{III} decreases from 75.8, the value determined for control nuclei (Fig. 1, thermograms e and f), to 72.4°C. The electrophoresis of the DNA fragments shows a sharp oligonucleosomal ladder (Fig. 3B, lane a); it can be seen that the mononucleosome represents the most probable fragment. This explains the marked decrease in T_m^{III}, since a large fraction of the linkers is cleaved under these digestion conditions, and it is quite obvious that an increase in the DNA free ends involves a depression of the denaturation temperature. Nuclei were then submitted to

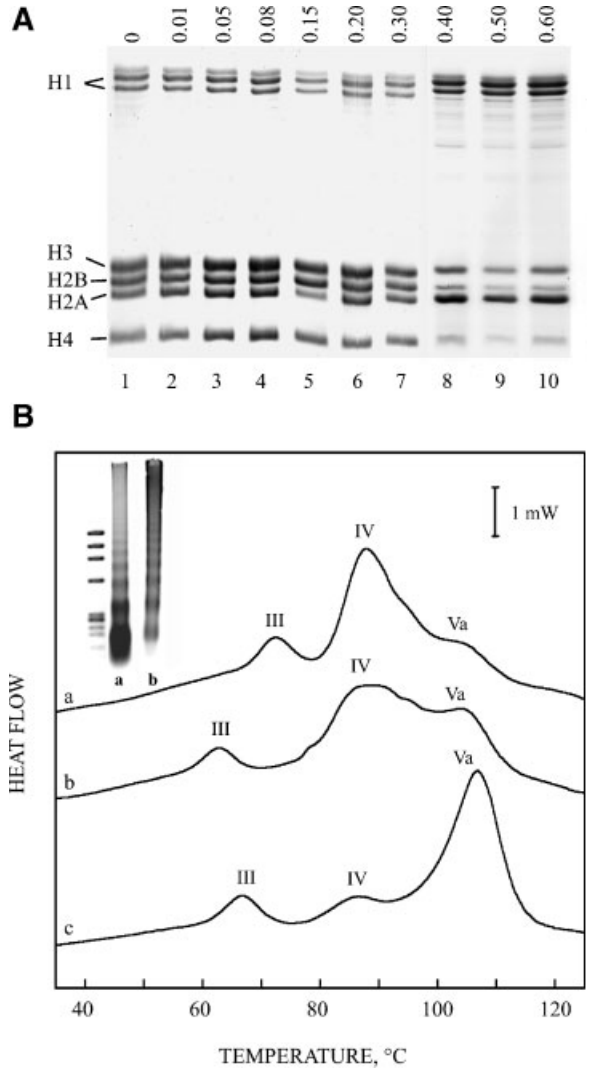

Fig. 3. Exposure of nuclear chromatin from calf thymus to KSCN does not involve histone dissociation upto 0.3 M (**A**) and unaffects the repeat length of the DNA fragments generated by MN digestion (**B**). A: Electrophoretic analysis of the histones which remain associated with DNA after equilibration of chromatin with the KSCN containing buffers used in the DSC experiments. The concentration of KSCN in mol/L is reported on the top of each lane. No change in the electrophoretic pattern is observed upto 0.3 M KSCN (**lanes 1–7**). The onset of dissociation occurs abruptly at 0.4 M (**lane 8**). Note, however, that no further histone dissociation is induced by raising KSCN concentration upto 0.6 M (**lanes 9**, **10**). B: The inset shows the electrophoretic pattern on 1.5% agarose gel of the DNA isolated from nuclear chromatin digested with 20 U/ml MN for 15 min at 37°C in digestion buffer (**lane a**) and with 50 U/ml for 1 h at 37°C in digestion buffer containing 0.2 M KSCN (**lane b**). The size marker is ΦX174/*HaeIII* fragments. The corresponding thermograms show that heterochromatin is almost completely degraded; note, however, that in the thermal profile determined in the presence of 0.2 M KSCN (b) T_m^{III} has an unusually low value (62.8°C) which shows that SCN^- binding and DNA cleavage additively destabilize the linker domain. The thermal profile of nuclei equilibrated in 0.2 M KSCN is reported for comparison (**c**).

digestion in the presence of 0.2 M KSCN (Fig. 3B, thermal profile b). Due to the strong destabilizing effect exerted by the salt on the tertiary structure of proteins [von Hippel and Schleich, 1969] partial inactivation of the enzyme occurs. In order to obtain an extent of digestion comparable with that observed in the absence of KSCN the concentration of MN was increased upto 50 U/ml and digestion carried out for 1 h. In Figure 3B, the thermal profile (b) is compared with that of undigested nuclei in 0.2 M KSCN (c). A dominant endotherm at 88°C and residual heterochromatin at ~104°C are apparent; interestingly, transition III occurs at 62.8°C, showing that the decrease in T_m^{III} with respect to the control (~13°C) additively reflects the effect of digestion (~3.4°C) and that of SCN^- binding (~9°C). The electrophoretic pattern of the DNA fragments shows that the exposure to SCN^- does not involve nucleosome sliding; comparable values of the repeat length were determined both in the presence (198 ± 7 (mean of three determinations ±SE), lane b) and in the absence (186 ± 7, lane a) of KSCN.

Overall the results reported in this section confirm the postulate that KSCN weakens histone–DNA interactions primarily by a charge suppression mechanism, at variance with other neutral salt which affect the electrostatic interactions in chromatin on a charge shielding basis [Conio et al., 1974]. As reported above the value of $\Delta T_m/\Delta$[KSCN] for transition III is ~−39 deg/M, to be compared with ~−20 deg/M determined for calf thymus chromatin in the presence of NaCl [Cavazza et al., 1991]; moreover, for transition IV we have found ~−28 deg/M in the case of KSCN, while T_m^{IV} is unaffected by NaCl concentration between 1 mM and 0.123 M. The analogy between anion binding and histone acetylation can be extended by taking into account a recent mechanism for the acetylation induced dissociation of the tails from core DNA. Banéres et al. [1997] have reported that both H3 and H4 adopt a helical conformation in the nucleosome. More recently, Wang et al. [2000] have shown that an increase in the α-helical content of the tails occurs for both nucleosome core particle and whole histone octamer in solution upon acetylation. These authors have pointed out that the increase in α-helix can result in a shortening of the span of interaction of core histone with DNA. This effect is expected to occur in the case of histone H4 as a consequence of acetylation of lysine 16 and

may be more pronounced in other histones such as H3 and H2B; these decrements in the span may cumulatively participate in the release of the flanking DNA regions that occurs upon acetylation, as experimentally observed. We suggest that this mechanism might be involved also in the release of the tails from DNA induced by SCN^-. Of course, an accurate representation of SCN^- binding would require a rigorous calculation of the electrostatic free energy of the region of the tail bound to DNA; we can, however, obtain a crude estimate of the fraction of lysines involved in the interaction with SCN^- by taking into account the values of the apparent binding constant (K^b_{app}) of SCN^- to the helical form of poly-L-lysine determined in a previous paper [Conio et al., 1974]. In 0.2 M KSCN K^b_{app} is equal to 2 M^{-1}. Since the molar concentration of the lysines located in the N-terminal domains of histones can be easily calculated, we can estimate the fraction of amino groups which interact with SCN^-. We obtain that approximately 29% of the positive charges is neutralized for each histone molecule; this value increase slightly (upto 37%) in 0.3 M KSCN. We conclude that the binding of SCN^- between 0 and 0.3 M can actually involve decreases in the positive charge which are sufficient for triggering the release of the histone tails.

The onset of dissociation occurs at 0.4 M KSCN (Fig. 2A, panel h): the abrupt conversion of $\Delta H_m{}^{Va}$ into $\Delta H_m{}^{Vb}$ shows that heterochromatin is undergoing unfolding. Due to the coexistence of native chromatin, naked DNA and free histones, it is almost impossible to deconvolve the thermal profile below ~90°C. The electrophoretic analysis of the histones which remain associated with the DNA after salt treatment, is shown in Figure 3A, lanes 8–10. A striking difference with respect to the well known dissociation mode induced by NaCl is apparent. Between 0.4 and 0.6 M KSCN H1 is not released, while it is fully dissociated in 0.6 M NaCl; moreover in 0.4 M KSCN 70, 65, and 50% H2B, H4, and H3, respectively, are dissociated from DNA. These values are not appreciably affected by increasing KSCN concentration upto 0.6 M.

This behavior can again be ascribed to the dominant charge neutralization effect exerted by SCN^-. Core histone dissociation begins at 0.4 M KSCN after the release of the tails, and is driven by the binding to the lysine groups placed on the globular domains; in the presence of simple electrolytes dissociation occurs at ~2 M, a concentration which is much higher than that determined for KSCN. The same effect has been observed in the case of the isolated core particle; using circular dichroism and stopped flow circular dichroism we have found that KSCN and NaCl dissociate the core particle at 0.45 and 2 M, respectively [D'Arrigo et al., unpublished results]. As reported above, the extent of dissociation of histone does not increase between 0.4 and 0.6 M; this trend depends on a compensating decrease of K^b_{app} (from 1 to 0.7 M^{-1}) induced by the charge shielding effect associated with the increase in KSCN concentration [Conio et al., 1974]. The detailed analysis of the dissociation of chromatin induced by KSCN should allow to determine the electrostatic free energy of interaction between histones and histones–DNA in the nucleosome, and therefore deserves further work.

Selective Trypsin Digestion Shows That in Euchromatin Both H1 and H3 Interact With Linker DNA, While Core DNA Is Stabilized by the Binding of H4

In the previous section, we have shown that the decrease in the stability of euchromatin induced by SCN^- reflects the loosening of the electrostatic binding of histone terminal domains to DNA. Which are the histones involved? The problem remains undetermined, since different histones are expected to be involved in the stabilization of the linker and core particle DNA. On the other hand, the tails which transiently lift off the DNA as a consequence of SCN^- binding, should show a marked increase in the rate of digestion by trypsin and therefore could be identified by comparing differential trypsin digestion experiments in the presence or absence of KSCN.

The thermograms of control nuclei and nuclei digested with 100 μg/ml for 80 min in DM are shown in Figure 4A, panels a and b, respectively; no significant difference is detectable. The electrophoretic analysis of the histone complement shows (Fig. 4A, panel f, lane 2) that trypsin treatment has digested ~80% H1 and ~50% H3; H2A, H2B, and H4 are not affected. It is important to note, however, that the globular domain of H1 (GH1) remains associated with chromatin (Fig. 4A, panel f, lane 2) [Leuba et al., 1998a]. The thermogram of nuclei digested and scanned in the presence of

0.2 M KSCN is reported in Figure 4A, panel d. T_m^{III} and T_m^{IV} decrease from 73.1 to 66.5 and from 91 to 85°C with respect to control nuclei (panel a); there is also a small decrease in ΔH_m^{Va}, showing that digestion induces partial unfolding of the heterochromatin domains. Under these conditions digestion of H3 and H4 increases upto 80% and 50%, respectively (panel f, lane 3); H2B shows a 20% decrease, while no appreciable depletion in H1 and H2A is observed with respect to the digestion in the absence of SCN^- (lane 2). The thermal profile of nuclei equilibrated with DM after trypsin digestion in KSCN is finally shown in Figure 4A, panel e. While refolding of heterochromatin occurs, as indicated by the increase in ΔH_m^{Va} at the expense of ΔH_m^{Vb}, the values of T_m^{III} and T_m^{IV} still show, in spite of the removal of the destabilizing effect of SCN^-, a significant decrease (4.6 and 3°C) with respect to those of native nuclei. Thus, digestion of 80% H1, 80% H3, and 50% H4 exerts a large effect on the stability of the linker and of core DNA in euchromatin.

For the purpose of an immediate comparison with our observations, in Table I are briefly reported data from very recent works on the structural role of linker and core histone tails. As far as linker DNA is concerned, our results are in remarkable agreement with previous ultrastructural observations of Leuba et al. [1998a,b]. These authors have shown that the stabilization of the extended structure of chromatin at low salt requires (i) the globular domain of H1, and (ii) either the tails of H1 or the N-terminal domain of H3. Likewise, for our chromatin samples, which retain the globular domain of H1 but not the tails, as a consequence of the SCN^- induced loosening of interactions with DNA, destabilization of the linker occurs when both H1 and H3 are extensively digested. Furthermore, core particle DNA destabilization is observed when 50% H4 is cleaved, in line with the results of Zheng and Hayes [2003b]. These authors, on the basis of crosslinking determinations in a dinucleosome model concluded that the N-terminal tails of H3 and H4 make exclusively intra-nucleosomal histone–DNA

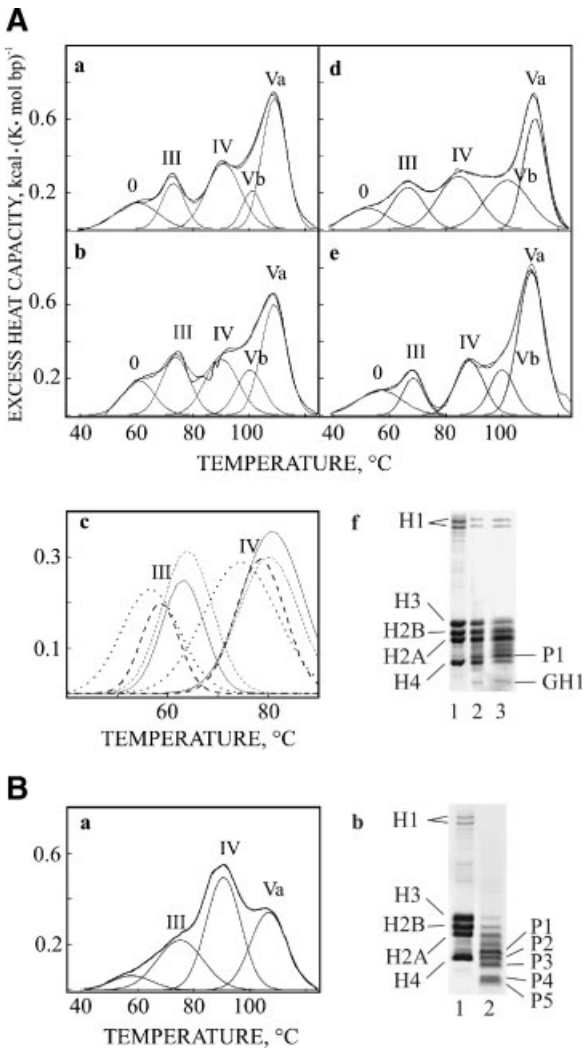

Fig. 4. **A**: Trypsin cleavage of the tail domains of H1 and of the N-terminal domain of H3 decreases the stability of the linker and of the core particle DNA in euchromatin. **a**: Control nuclei scanned in DM. **b**: Nuclei digested with 100 μg/ml trypsin for 80 min in DM or (**d**) in the presence of 0.2 M KSCN; either samples was directly scanned in the buffer used for digestion. **e**: Nuclei digested in the presence of 0.2 M KSCN and re-equilibrated with DM. For a better appreciation of the changes induces by trypsin digestion, an enlargement of the low temperature region of the deconvolved thermograms, showing only endotherms III and IV is reported in (**c**); (—), (- - -), (· · · ·), and (– –) correspond to the excess heat capacity profiles shown in panels a, b, d, and e, respectively. **f**: Sixteen percent SDS–PAGE characterization of the histone complement of native nuclei (**lane 1**), of nuclei digested in DM (**lane 2**), and in 0.2 M KSCN (**lane 3**) as described above. The migrations of the linker and of core histones, as well as of the globular domains of H3 (P1) and H1 (GH1) are indicated. **B**: Cleavage of H2A, H2B, and H4 induces heterochromatin unfolding. **a**: Deconvolved heat capacity curves of nuclei extensively digested with 15 μg/ml trypsin for 15 h in DM. Note that transition V_b is no longer observed, indicating that V_a directly converts into IV according to an all-or-none (two state) transition [Balbi et al., 1999]. The electrophoretic patterns of histones which remain associated with DNA in native chromatin and after trypsin digestion are shown in (**b**), **lanes 1** and **2**. P1, P2, P3, and P4 + P5 indicate the trypsin resistant peptides of H3, H2A, H2B, and H4, respectively.

TABLE I. Binding Sites and Functions of Histone Terminal Domains According to Recent Literature Data

Histone terminal tail	Binding site	Suggested function
H1 C and N-terminal tails	Linker DNA in extended chromatin at low ionic strength	Close packing of adjacent nucleosomes, Leuba et al. [1998a,b]
H3 N-terminal tail	Linker DNA in extended chromatin at low ionic strength	Stabilization of the three-dimensional structure of extended chromatin, Leuba et al. [1998a,b]
H2A, H2B N-terminal tails	DNA from the neighboring nucleosome in a model dinucleosome	Chromatin condensation, Zheng and Hayes [2003b]
H3, H4 N-terminal tails	DNA from the same nucleosome in a model dinucleosome	Regulation of DNA accessibility at the nucleosome level, Zheng and Hayes [2003a,b]
H4 N-terminal tail	Region of extreme acidity on the exposed face of the H2A-H2B dimer from an adjacent nucleosome	Chromatin condensation, Dorigo et al. [2003]
H2A C-terminal tail	DNA at the dyad axis or near the periphery of a reconstituted nucleosome in the absence or presence of linker DNA, respectively	Maintenance of different functional states of chromatin fiber, Lee and Hayes [1998]

contacts (Table I). In addition to these recent observations, early work from different laboratories has provided evidence of the intra-core binding of the N-tail of H4 in decondensed chromatin. Using proton NMR spectroscopy, Walker [1984] has found that the basic tails of core histone are linked to core DNA in core chromatin; dissociation occurs between 0.2 and 0.6 M NaCl. Moreover, the selective removal of the tails of H3 and H4 or of H2A and H2B induces dramatic changes in the thermal denaturation profile of the isolated core particle [Ausió et al., 1989] showing that the central region of core DNA interacts with the tails of H4.

Very recently, Dorigo et al. [2004] using a precise disulfide cross-linking technique have suggested that the folding of nucleosome arrays into the 30 nm fiber is directed by the inter-core interaction of the N-terminal domains of H4 with H2A. Is this postulated role of H4 in contradiction with our finding that N-terminal domain of this histone is bound to core DNA in euchromatin? The answer is no. We recall that transition IV results from the melting of the core particles placed within an extended (euchromatin) domain [Balbi et al., 1989]; this subpopulation does not undergo salt induced condensation, as a consequence of the binding of trans active factors and/or of specific interactions with the nuclear matrix [Barboro et al., 1993]. The amount of euchromatin is expected to be related within the number of genes which are at work in a given cell type; since this number is almost the same in all of resting cells, we can explain why ΔH_m^{IV} represents a fixed fraction ($\sim$0.3) of the total denaturation enthalpy of nuclear chromatin [Cavazza et al., 1991]. In the extended conformation of euchromatin the core particles are at distances much higher than the length of the tail of H4, so preventing the latter from establishing inter-core interactions. The situation is, however, very different for inactive heterochromatin, which undergoes reversible ionic strength dependent condensation–decondensation [Cavazza et al., 1991]. In this case the binding of H1 [Russo et al., 1995] and H3 to linker DNA, could involve both a progressive decrease in the inter-core distance [Leuba et al., 1998a] and subtle changes in the conformation of the dinucleosome, so allowing the basic tail of H4 to interact with an acidic aminoacid patch placed on an adjacent nucleosome [Dorigo et al., 2004]. This event could represent the nucleation step of the higher order structure. Our experiments indicate that, when chromatin is digested with 100 μg/ml trypsin for 80 min (Fig. 4A, panel d), $\sim$50% of H4 is cleaved; therefore, at this stage proteolysis occurs also inside the heterochromatic domains. The occurrence of proteolysis is not detectable on inspection of the high temperature endotherms in the DSC profile of digested nuclei, which reflect changes in the interactions of DNA with histones in heterochromatin, but will directly affect transition 0 in which the histone octamer unfolds. Indeed, the comparison between the value of T_m^0 in native nuclei (60°C) and in nuclei digested with trypsin in the presence of 0.2 M KSCN (Fig. 4A, panels a and e, respectively) shows this effect, since in the latter case T_m^0 drops to 57.5°C; this small but significant decrease has been confirmed by careful determination of T_m^0 in different samples (data not shown).

Heterochromatin Formation Requires the Internucleosomal Binding of H4, H2A, and H2B

In this section, we show that a direct link exists between definite changes in the digestion pattern of histones and the stability of heterochromatin. However, it might be difficult to correlate immediately the complex changes in the pattern of histone digestion with the many modifications induced in the thermal profile. Therefore, in Figure 5 we compare the fractions of states, namely, the fractions of core particles which denature in transition IV, V_b, and V_a, respectively [Russo et al., 1995] with the percentages of digested histones; either set of data is plotted as a function of R, the cumulative fraction of digested histones. For example, for $R = 0.46$ we find that 80% of H3 has been digested, while fV_a, which corresponds to the fraction of heterochromatin, is ~ 0.5.

The data reported in Figure 4A, panel d indicate that the 30 nm fiber shows incipient unfolding in DSC experiments carried out in 0.2 M KSCN when 80% H1, 80% H3, 50% H4, and 20% H2B are digested by trypsin (Fig. 5, $R = 0.46$). On the other hand, in a previous paper, we have reported that digested chromatin samples in which the histone tails have been fully removed show the thermal profile characteristic of the unfolded state (see Fig. 7 in Cavazza et al. [1991]); only transitions III and IV at 76 and at 90°C are observed (Fig. 5, $R = 1$), while ΔH_m^{III} increases indicating that the fraction of DNA which melts in this endotherm also increases, in agreement with early observation by Allan et al. [1982]; these authors have shown that after complete digestion of H1 and of core histones approximately 56 base pairs of DNA are released from the core particle. Thus, unfolding of the higher order structure is expected to occur synchronous with the degradation of H2B and/or H2A and/or residual H4. This result is just shown in Figure 4B, which reports the heat capacity curve of nuclei digested with 15 μg/ml trypsin for 15 h at 4°C. Endotherm IV, corresponding to the denaturation of core DNA in extended chromatin, dominates the thermogram; transition V_b, which result from the denaturation of core DNA in the isolated 30 nm fiber, disappears while an appreciable (40%) fraction of heterochromatin (aggregated 30 nm fibers) is still observed (transition V_a). At this stage 100%, 89%, 83%, 62%, and 65% of H1, H3, H2B, H2A, and H4, respectively, have been digested (Fig. 4B, panel a, lane 2 and Fig. 5, $R = 0.80$). Thus, both decondensation of the fiber and extensive unfolding of heterochromatin are induced by a limited increase in the fraction of digested H4 (from 50% to 65%) and by the extensive removal of the N-terminal domains of H2B and H2A (80% and 62%, respectively).

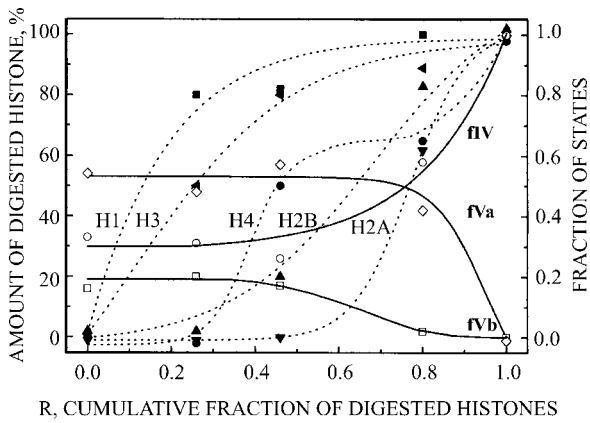

Fig. 5. Diagram showing the correlation between the fraction of states, namely the fraction of core particles denaturing in IV, V_a, and V_b, and the extent of digestion of each histone (right and left ordinate, respectively). The fraction of states has been obtained by normalizing the experimental values of ΔH_m^{IV}, ΔH_m^{Va}, ΔH_m^{Vb} by the total enthalpy change ($\Delta H_m^{IV} + \Delta H_m^{Va} + \Delta H_m^{Vb}$). In order to facilitate the interpretation of the results the trend of the thermodynamic parameters (solid lines) and of the amount of digested histones (dotted lines) are plotted as a function of R, the cumulative fraction of digested histones. The values of R equal to 0.26, 0.46, and 0.80 correspond to the digestion experiments shown in Figure 4A panels b, e and Figure 4B panel a, respectively. Note that the digestion of H4 occurs according to a biphasic mechanism: at $R = 0.46$, 50% of the histone H4 has been digested, resulting in a appreciable decrease in the stability of euchromatin. Above $R = 0.46$ H4 digestion occurs inside the higher order structure; as discussed in the text, transition V_b disappears and chromatin decondensation involve only two states: heterochromatin (transition V_a) and extended chromatin (transition IV). (■) H1, (◀) H3, (●) H4, (▲) H2B, (▼) H2A, (○) fIV, (◇) fV_a, (□) fV_b.

The correlation between H4 digestion and decondensation of the 30 nm fiber is in agreement with recent results by Dorigo et al. [2004] as discussed above. Furthermore, a previous report from the same laboratory [Dorigo et al., 2003] suggested that the tails of H2A and H2B are involved in several functions distinct from the condensation of the 30 nm fiber, such as the formation of links between separate fibers. Our data support this hypothesis, since a sudden decrease in the heterochromatin content is correlated with the digestion of H2B and H2A. In addition, for $R > 0.80$ fV_b is equal to 0, so that we observe the direct conversion of state V_a into

state IV, namely, of heterochromatin into euchromatin in the absence of the intermediate state V_b, in agreement with a previous thermodynamic study from our laboratory [Balbi et al., 1999] which has shown that heterochromatin formation is confined to the loop and involves highly cooperative (all-or-none) transition.

The highly cooperative nature of heterochromatin formation can be understood at molecular level by considering that this process requires not only the interaction of N-terminal tail of H4 with the core of H2A, which stabilizes the single 30 nm fiber, but also the formation of additional links with adjacent fibers possibly through the terminal domains of H2A and H2B. Thus, the high connectivity, rather than the absolute value of the free energy of formation, of an extended three dimensional network of histone–histone and histone–DNA contacts, could be responsible of the stability of silenced (heterochromatin) domains in resting cells. Of course, this conclusion does not absolutely rule out that silencing proteins such as SIR3 bind at specific sites in the higher order structure of chromatin, so providing the latter with an additional source of stabilization [Luger et al., 1997].

Work is in progress in our laboratory, using transmission electron microscopy of chromatin reconstituted with tail depleted H2A and/or H2B, in order to distinguish their structural role in heterochromatin stabilization.

REFERENCES

Allan J, Harborne N, Rau DC, Gould H. 1982. Participation of core histone "tails" in the stabilization of chromatin solenoid. J Cell Biol 93:285–297.

Ausió J, Dong F, van Holde KE. 1989. Use of selectively trypsinized nucleosome core particles to analyze the role of the histone "tails" in the stabilization of the nucleosome. J Mol Biol 206:451–463.

Balbi C, Abelmoschi ML, Gogioso L, Parodi S, Barboro P, Cavazza B, Patrone E. 1989. Structural domains and conformational changes in nuclear chromatin: A quantitative thermodynamic approach by differential scanning calorimetry. Biochemistry 28:3220–3227.

Balbi C, Sanna P, Barboro P, Alberti I, Barbesino M, Patrone E. 1999. Chromatin condensation is confined to the loop and involves an all-or-none structural change. Biophys J 77:2725–2735.

Banéres JL, Martin A, Parello J. 1997. The N tails of histones H3 and H4 adopt a highly structured conformation in the nucleosome. J Mol Biol 273:503–508.

Barboro P, Pasini A, Parodi S, Balbi C, Cavazza B, Allera C, Lazzarini G, Patrone E. 1993. Chromatin changes in cell transformation: Progressive unfolding of the higher-order structure during the evolution of rat hepatocyte nodules. A differential scanning calorimetry study. Biophys J 65:1690–1699.

Barboro P, Alberti I, Sanna P, Parodi S, Balbi C, Allera C, Patrone E. 1996. Changes in the cytoskeletal and nuclear matrix proteins in rat hepatocyte neoplastic nodules in their relation to the process of transformation. Exp Cell Res 225:315–327.

Ben-Haïm E, Lesne A, Victor JM. 2001. Chromatin: A tunable spring at work inside chromosomes. Phys Rev E 64:051921-1–051921-19.

Cavazza B, Brizzolara G, Lazzarini G, Patrone E, Piccardo M, Barboro P, Parodi S, Pasini A, Balbi C. 1991. Thermodynamics of condensation of nuclear chromatin. A differential scanning calorimetry study of the salt-dependent structural transitions. Biochemistry 30:9060–9072.

Chipev CC, Angelova MI. 1983. Temperature dependence of the transition enthalpy of core particle DNA and of long DNA. Int J Biol Macromol 5:252–253.

Conio G, Patrone E, Rialdi G, Ciferri A. 1974. Polyelectrolytes in salt solutions. Quantitative separation of binding and electrostatic effects for poly(L-ornithine) and poly(L-lysine). Macromolecules 7:654–659.

Dorigo B, Schalch T, Bystricky K, Richmond TJ. 2003. Chromatin fiber folding: Requirement for the histone H4 N-terminal tail. J Mol Biol 327:85–96.

Dorigo B, Schalch T, Kulangara A, Duda S, Schroeder RR, Richmond TJ. 2004. Nucleosoma arrays reveal the two-start organization of the chromatin fiber. Science 306: 1571–1573.

Felsenfeld G. 1996. Chromatin unfolds. Cell 86:13–19.

Gavazzo P, Vergani L, Mascetti GC, Nicolini C. 1997. Effects of histone acetylation on chromatin structure. J Cell Biochem 64:466–475.

Labarbe R, Flock S, Maus C, Houssier C. 1996. Polyelectrolyte counterion condensation theory explains differential scanning calorimetry studies of salt-induced condensation of chicken erythrocyte chromatin. Biochemistry 35:3319–3327.

Laemmli UK. 1970. Cleavage of structural proteins during the assembly of the head of bacteriophage T4. Nature (Lond) 227:680–685.

Lee KM, Hayes JJ. 1998. Linker DNA and H1-dependent reorganization of histone–DNA interactions within the nucleosome. Biochemistry 37:8622–8628.

Leuba SH, Bustamante C, Zlatanova J, van Holde K. 1998a. Contributions of linker histones and histone H3 to chromatin structure: Scanning force microscopy studies on trypsinized fibers. Biophys J 74:2823–2829.

Leuba SH, Bustamante C, van Holde K, Zlatanova J. 1998b. Linker histone tails and N-tails of histone H3 are redundant: Scanning force microscopy studies of reconstituted fibers. Biophys J 74:2830–2839.

Luger K, Mäder AW, Richmond RK, Sargent DF, Richmond TJ. 1997. Crystal structure of the nucleosome core particle at 2.8 Å resolution. Nature 389:251–260.

Maniatis T, Fritsch EF, Sambrook J. 1982. Molecular cloning: A laboratory manual Cold Spring Harbor Laboratory. New York: Cold Spring Harbor.

Nicolini C, Trefiletti V, Cavazza B, Cuniberti C, Patrone E, Carlo P, Brambilla G. 1983. Quaternary and quinternary structures of native chromatin DNA in liver nuclei: Differential scanning calorimetry. Science 219: 176–178.

Panyim S, Bilek D, Chalkey R. 1971. An electrophoresis comparison of vertebrate histones. J Biol Chem 246: 4206–4215.

Reuter G, Giarre M, Farah J, Gausz J, Spierer A, Spierer P. 1990. Dependence of position-effect variegation in *Drosophila* on dose of gene encoding an unusual zinc-finger protein. Nature (Lond) 344:219–223.

Russo I, Barboro P, Alberti I, Parodi S, Balbi C, Allera C, Lazzarini G, Patrone E. 1995. Role of H1 in chromatin folding. A thermodynamic study of chromatin reconstitution by differential scanning calorimetry. Biochemistry 34:301–311.

Solt D, Farber E. 1976. New principle for the analysis of chemical carcinogenesis. Nature (Lond) 263:701–703.

Spadiliero B, Nicolini C, Mascetti G, Henriquez D, Vergani L. 2002. Chromatin of *Tripanosoma cruzi*: In situ analysis revealed its unusual structure and nuclear organization. J Cell Biochem 85:798–808.

Teif VB, Haroutiunian SH, Vorob'ev VI, Lando DY. 2002. Short-range interactions and size of ligands bound to DNA strongly influence adsorptive phase transition caused by long-range interactions. J Biomol Struct Dyn 19:1–8.

van Holde KE. 1988. Chromatin. New York: Spring-Verlag.

von Hippel PH, Schleich T. 1969. The effect of neutral salts on the structure and conformational stability of macromolecules in solution. In: Timasheff SN, Fasman GD, editors. Structure and stability of biological macromolecules. New York: Marcel Dekker, Inc. pp 417–576.

Walker IO. 1984. Differential dissociation of histone tails from core chromatin. Biochemistry 23:5622–5628.

Wang X, Moore SC, Laszckzak M, Ausió J. 2000. Acetylation increases the α-helical content of the histone tails of the nucleosome. J Biol Chem 275:35013–35020.

Weintraub H. 1985. Tissue-specific gene expression and chromatin structure. Harvey Lect 79:217–244.

Zheng C, Hayes JJ. 2003a. Structures and interactions of core histone tail domains. Biopolymers 68:539–546.

Zheng C, Hayes JJ. 2003b. Intra- and inter-nucleosomal protein–DNA interactions of the core histone tail domains in a model system. J Biol Chem 278:24217–24224.